Mechanics of Advanced Composite Structures 9 (2022) 367 – 376

Semnan University

Mechanics of Advanced Composite Structures

journal homepage: http://MACS.journals.semnan.ac.ir

The Effect of Al Additive and Arc Melting Time on Synthesis of Ti_3SiC_2 MAX Phase using Ti/SiC/Al/Graphite

A. Moradkhani [a*], B.S. Kozekanan [b], H. Baharvandi [c]

[a] *Faculty of Mechanical Engineering, Shahid Rajaee Teacher Training University, Tehran, Iran*
[b] *Department of Mechanical Engineering, University of Tabriz, Tabriz, Iran*
[c] *Department of Materials Engineering, University of Tehran, Tehran, Iran*

KEYWORDS

MAX phase;
Arc-melting method;
Ti_3SiC_2;
Aluminum.

ABSTRACT

In this study, the effect of different molar ratios of primary powders and arc melting setting time on the synthesis of Ti_3SiC_2 powder has been investigated. For this purpose, Silicon Carbide (SiC), Titanium (Ti), graphite (C) and aluminum (Al) powders with molar ratios of 3Ti:1.2SiC:0.8C, 3Ti:1.2SiC: 0.8C:0.1Al and 3Ti:1.2CiC:0.8C:0.3Al were mixed by a planetary mill under an argon atmosphere for 5h. The resulting mixture was formed with a press and subjected to arc melting at 1, 3, 5, and 10s. In samples containing Al additive, the purity of Ti_3SiC_2 increases with increasing arc melting setting time up to 5s, and the purity decreases with increasing the arc time. The best result was obtained in the sample 3Ti:1.2SiC:0.8C:0.1Al containing 83.6 wt% of Ti_3SiC_2, which was obtained during the 5s arc melting.

1. Introduction

Max phases have dual behaviors of the properties of metals and ceramics [1]. They show a set of excellent properties such as good machinability, and good thermal and electrical conductivity [2]. They are resistant to thermal shocks and retain their properties at high temperatures under dynamic load conditions. Like ceramics, they are refractory and resistant to oxidation and have a relatively low density. Due to these unique properties, MAX phases are used for high-temperature applications, protective coatings, sensors, low friction surfaces, electrical connections, adjustable films for microelectromechanical systems, and other applications [3-6].

One of the most famous families of MAX phases is Ti_3SiC_2, which has unique mechanical properties. It has outstanding properties such as high Young's modulus (320 GPa), low density (≈4.54 gr/cm^3), excellent corrosion and chemical resistance, and high melting point (3000˚K) [7]. Ti_3SiC_2 has high electrical and thermal conductivity (4.5×10^6 $\Omega^{-1}m^{-1}$, and 43 $wm^{-1}k^{-1}$, respectively), low hardness (4 GPa), resistance to thermal shocks, and the ability to convert to complex shapes by machining [7-10]. Ti_3SiC_2 is brittle at room temperature and plastically deforms at temperatures above 1200˚C [11]. At 1300° C and in the vicinity of air, its yield stress in the state of tension and pressure is 100 and 500 MPa, respectively [12].

Ti_3SiC_2 MAX phase is prepared from various methods such as Mechanical Alloying (MA) [13], Spark Plasma Sintering (SPS) [14-17], Pressureless Sintering (PS) [18-23], Self-Propagating High-Temperature Synthesis (SHS) [24 -25], Infiltration [26, 27], Pulse discharge Sintering (PDS) [28-29], Combustion Synthesis Method [30], Hot Pressing (HP) [31,32], Hot Isostatic Pressing (HIP) [33] , Chemical Vapor Deposition (CVD) [34], Pulse Discharge Plasma Sintering (PDS) [35, 36], Solid State Reaction [37], Reactive Melt Infiltration (RMI) [38], Pressure-assisted Self-propagating High-temperature Synthesis (PSHS) [25], Gas-Pressure Combustion Synthesis (GPCS) [39], solid-liquid reactions [40] and arc melting technique [41]. Furthermore, different combinations of primary powders such as Ti/Si/C, Ti/Si/TiC, Ti/SiC/Si/TiC, TiH_2/Ti/SiC/C, Ti/Si/TiC/Al,

* Corresponding author. Tel.: +98-9125907184; Fax: +98-21-22970033
E-mail address: alireza.moradkhani@sru.ac.ir

DOI: 10.22075/macs.2022.23581.1342
Received 2021-06-02; Received in revised form 2022-08-18; Accepted 2022-09-20.

Ti/SiC/TiC/Al and Ti/polycarbosilane have been used as raw materials in manufacturing methods. In addition, in most cases, the synthesized products have secondary phases of TiC, $TiSi_2$, and Ti_5Si_3 as impurities [37].

Abu et al [41] used a mixture of 3Ti:Si:2C as the primary powders and the process was carried out by an arc melting device with an arc current of 90A for 3 to 90s under a pure argon gas atmosphere. The results showed that with the purity of Ti_3SiC_2, synthesized during 5s, the arc setting reached 86.9 wt%, which is an acceptable value compared to pressure-less self-combustion synthesis methods.

Chemical properties and Physical are the most significant characteristics of the Ti2AlC MAX phase, which have introduced this material as the most practical MAX phase known so far. This Ti2AlC with a density of 4.11 g/cm^3 is recognized as the lightest Ti-base MAX phase of the 211 series [42]. The values of hardness, thermal conductivity, and electrical conductivity of this ternary carbide are obtained as 4-5 GPa, 46 W/mK, and, $2.8\times10^6\ \Omega^{-1}.m^{-1}$ at room temperature, respectively [29].

In the present study, the synthesis of Ti_3SiC_2 was studied using raw materials including Ti/SiC/Al/graphite with molar ratios of 3Ti:1.2SiC:0.8C, 3Ti:1.2SiC:0.8C:0.1Al and 3Ti:1.2SiC:0.8C:0.3Al and using arc melting technique. The specific aim of this study was to find the optimal values of arc melting time parameters, which are barely possible to be found in other articles, and to explore methods related to the calculation of this vital parameter in the sintering process. Furthermore, exploring the mixing ratio of raw materials and the effect of Al additive in the synthesis of Ti_3SiC_2 powder is explained.

2. Materials and methods

The Ti powder (HDH, gas atomized) in this investigation with a particle size of less than 40μm and purity of more than 99 wt% was made by Merck Co. Fig. 1 shows the SEM image of the Ti powder. Fig. 2 also shows the XRD pattern of Ti powder.

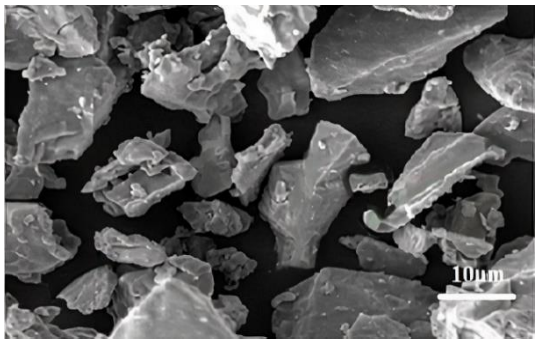

Fig. 1. SEM of titanium powder

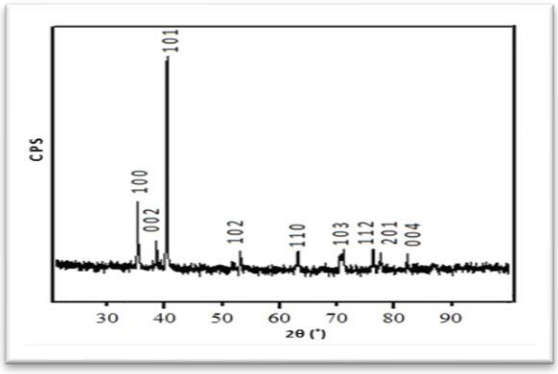

Fig. 2. XRD pattern of Ti powder

The utilized A1 powder with 99 wt% purity, made by Merck Co., has an average particle size of 30μm. Figures 3(a) and 3(b) show the SEM image of the morphology and particle size Analyzer (PSA) of Al powder, respectively. Fig. 4 shows the XRD pattern of Al powder.

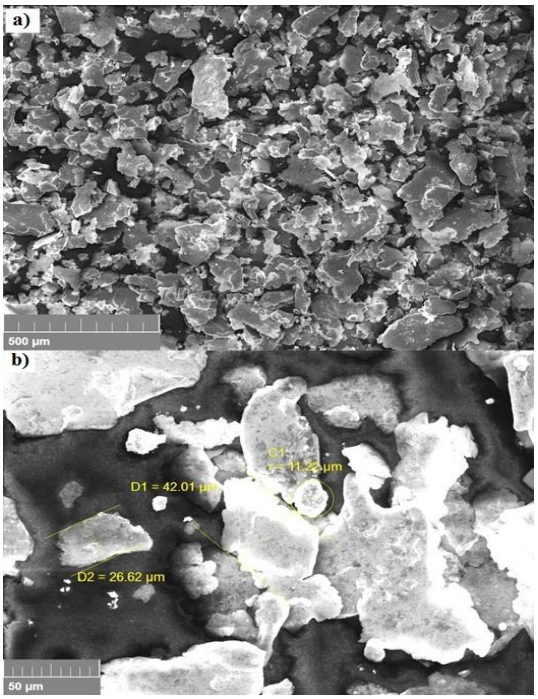

Fig. 3. SEM image of powder Al (a) morphology and (b) PSA

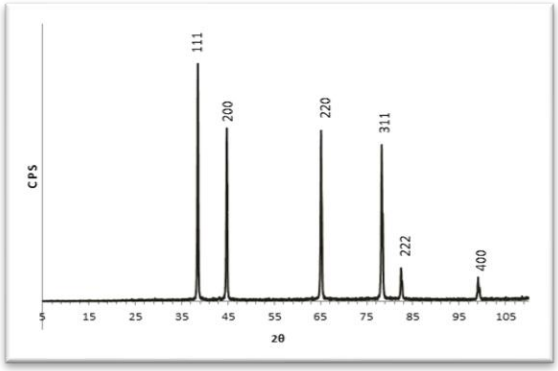

Fig. 4. XRD pattern of Al powder

The SiC powder, made by Merck Co., used is also with a particle size of less than 10µm (50 d50 = 5.65) and with a purity of 98%. Fig. 5(a) shows the SEM image of SiC powder and Fig. 5(b) shows its PSA analysis. Fig. 6 also shows the XRD pattern of the primary SiC powder.

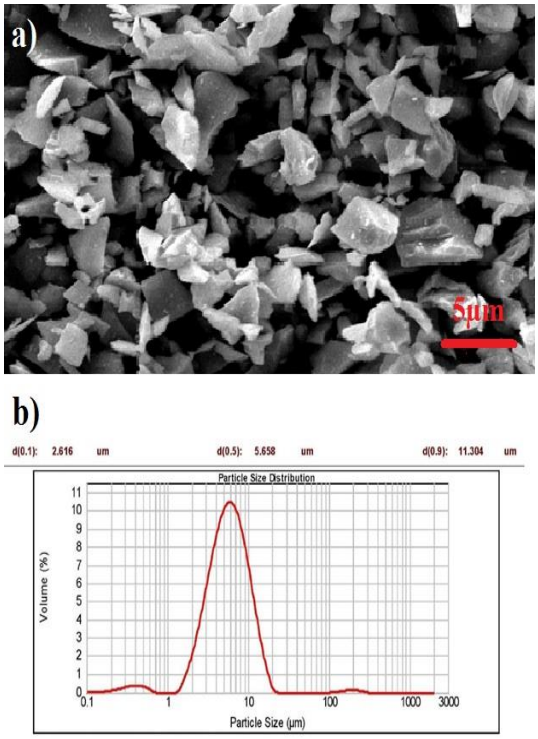

Fig. 5. (a) SEM image of SiC powder (b) Particle size analysis (PSA) of SiC powder

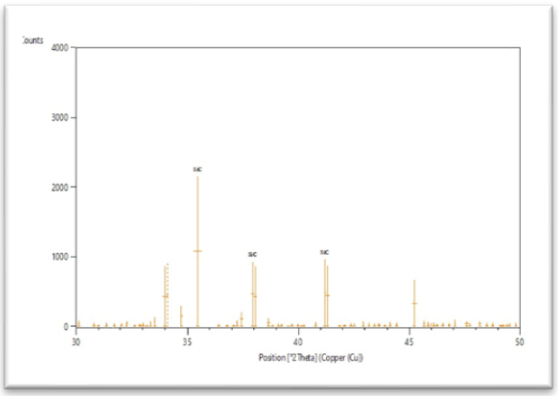

Fig. 6. XRD pattern of SiC powder

The graphite powder used by Sigma-Aldrich Co. has a particle size of less than 100µm and purity of more than 99wt%. Fig. 7(a) shows the morphology of graphite powder particles and Fig. 7(b) shows PSA, which is in the range of 8-30µm. Fig. 8 also illustrates the XRD pattern of graphite powder.

The primary powders were mixed with different molar ratios for the synthesis of Ti_3SiC_2 according to Table 1. Weight percentage is visible.

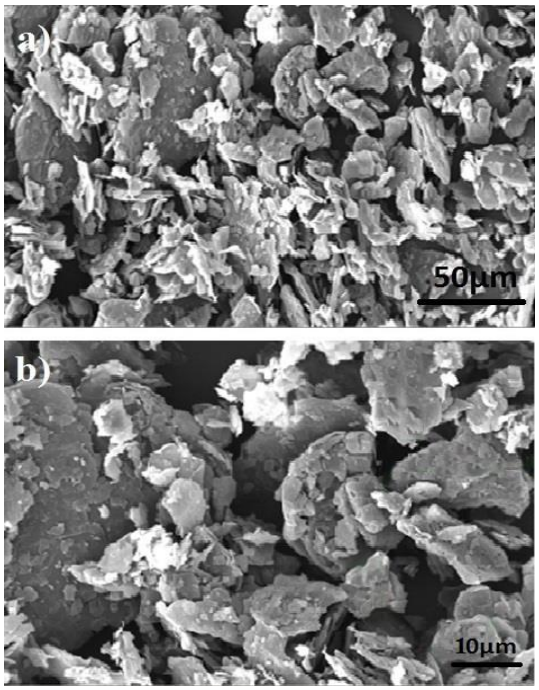

Fig. 7. Graphite powder SEM image (a) Particle morphology (b) Particle size

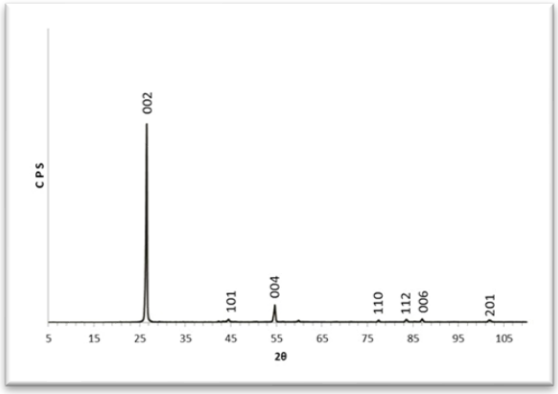

Fig. 8. XRD pattern of graphite powder

Table 1. Composition of raw materials for the synthesis of Ti_3SiC_2

No	molar ratio				%wt.			
	Ti	Si	C	Al	Ti	Si	C	Al
1	3	1.2	0.8	0	71.34	23.88	4.78	0
2	3	1.2	0.8	0.1	70.4	23.58	4.7	1.32
3	3	1.2	0.8	0.3	68.8	22.96	4.58	3.86

After initial weighing, the powders were mixed together in a certain molar ratio and then grind. The powder milling process was performed in a planetary mill at a speed of 200rpm in an argon gas atmosphere with a purity of 99.99% for 5h. For improving the contact between the particles and enhancing the reaction during heat treatment, the powder mixtures were pressed into tablets. To do this, the powders were placed in a steel mold with a diameter of 1.2 cm and subjected to a single-axis press with a pressure of 200 MPa for 15s.

The resulting pieces were placed on graphite plates inside the arc chamber and an arc melting of 100A current was applied to the samples in an argon gas atmosphere for 1, 3, 5, and 10s. Also, for a better comparison of the results, arc melting was applied to 3Ti:1.2SiC:0.8C:0.1Al sample for 15S with a current of 100A. After heat treatment, the synthesized parts were crushed with a mortar and the resulting powders were subjected to phase identification and microstructural analysis. Table 2 shows the sample code based on the amount of powder combination and the duration of the arc melting application.

Table 2. Basic combination and arc time applied to the samples

Sample No.	Basic combination	Arc time
1	3Ti:1.2SiC:0.8C	1
2		3
3		5
4		10
5	3Ti:1.2SiC:0.8C:0.1Al	1
6		3
7		5
8		10
9		15
10	3Ti:1.2SiC:0.8C:0.3Al	1
11		3
12		5
13		10

To weigh the powders, a digital scale made by Sartorius model BL1500S with an accuracy of 0.01gr was used. To mix and activate the surface of the powders which were used, a planetary mill made by the German company Fritsch, the Pulverisette model with a tungsten carbide (WC) chamber containing 15 bullets of zirconia was applied. To identify the phases, the XRD pattern of powders prepared in the range 2θ = 20˚-80˚ with 0.026 Step Size was used. The XRD device which was applied has been manufactured by Philips Co. model XPert PRO MPD, PANalytical with copper anode and equipped with Position Sensitive Detector and wavelength λ = 1.54Å. In this detector, the Active length is equal to 2θ= 3.35˚ and the stop time per step is 58s. Phase peaks were identified and their area was measured, finally, the weight percentages of Ti_3SiC_2 and TiC were calculated using equations 1 and 2.

$$W_{TiC} = \frac{I_{TiC}/I_{TSC}}{1.8+(I_{TiC}/I_{TSC})} \quad (1)$$

$$W_{TSC} = \frac{1.8}{1.8+(I_{TiC}/I_{TSC})} \quad (2)$$

in which W_{TiC} and W_{TSC} represent the weight percentages of TiC and Ti_3SiC_2, respectively, and I_{TiC} and I_{TSC} represent the level below the peak (200) TiC and peak (104) Ti_3SiC_2 [18, 43].

The microstructure images of the final compounds were prepared by Field Emission Scanning Electron Microscopes (FE-SEM) of TESCAN MIRA3-XM. This device is equipped with a reverse electron detector and a secondary electron.

3. Results and discussion

3.1. Effect of arc time on Ti_3SiC_2 synthesis

The XRD pattern of samples containing 3Ti:1.2SiC:0.8C at different time intervals under the arc melting is shown in Fig. 9. As can be seen, peaks of Ti_3SiC_2 phase are obvious in all samples. The main peak of the Ti_3SiC_2 phase is 2θ=39.5˚. TiC phase peaks are also seen as the main impurity in all samples. The main peak of TiC is 2θ=41.8˚. Since the combination of Ti_3SiC_2 is obtained from the reaction between the eutectic fluid and TiC [19], it is very difficult to avoid the formation of impurities, especially TiC, for reasons such as low synthesis temperature, lack of eutectic fluid, impurity of raw materials or contamination of the working environment (presence of carbon due to the use of graphite plant) [20]. Considering the X-ray diffraction pattern of Si and Ti in Fig 9 and the position of $TiSi_2$ on the left side of the diagram close to Si, it can be estimated that the Si in the initial powder is high and the excess Si reacts with Ti to form $TiSi_2$. This is in line with the findings of Sun and Yang [44], which exacerbate the excessive increase in Si and the formation of Ti silicides such as $TiSi_2$.

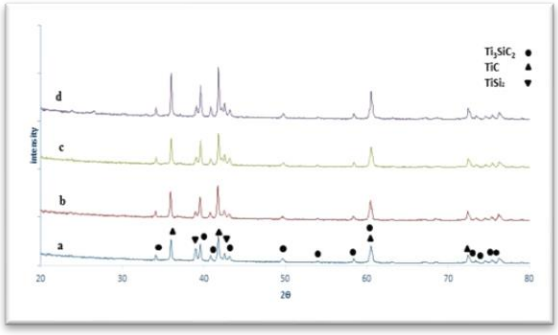

Fig. 9. XRD pattern of 3Ti:1.2SiC:0.8C mixture under arc melting at a) 1, b) 3, c) 5 and d) 10s

If figures or graphs are duplicated from other references, a citation should appear at the end of the caption.

3.2. Effect of Al on Ti_3SiC_2 synthesis

The XRD pattern of samples containing 3Ti:1.2SiC:0.8C:0.1Al under arc melting time of 1, 3, 5, 10, and 15s is shown in Fig. 10. As can be seen, with increasing arc melting time, the peak intensities of Ti_3SiC_2 and TiC increased. In fact, as the arc time increases, more particles react with

each other to form a more eutectic liquid phase, resulting in more Ti_3SiC_2 and TiC. It seems that the method of self-combustion synthesis during 1S arc melting time alone cannot be a suitable method to obtain high-purity Ti_3SiC_2 from Ti, SiC, and graphite raw materials. This is also consistent with the results of Yeh *et al* [24]. They found that high temperature and short time in the self-combustion synthesis method did not lead to the formation of single-phase Ti_3SiC_2. Also, the presence of Al in the basic combination can help to form the Ti_3SiC_2 phase. Due to the low melting temperature of Al, the Ti_3SiC_2 phase can germinate and then grow there, accelerating its formation. Due to the similarity of the XRD pattern results for arc times of 1, 3, 5, and 10s, the arc time of 15s has also been investigated. In Fig. 10 the intensity of the main peak of Ti_3SiC_2 (104) and the main peak of TiC (200) is almost constant with increasing arc time up to 5s. After the arc is settled, the existing Al melts in the powder mixture and fills the voids between the particles, improving mass and heat transfer between the particles. As mass and heat transfer improve, the reaction between Ti and carbon increases, and TiC formation accelerates. Since the formation of TiC is exothermic, it affects the synthesis reactions of the final product; However, this exothermic reaction complicates the temperature control of Ti_3SiC_2 synthesis [46,47]. Figures 10-d and 10-e show the reduction of the main peak of Ti_3SiC_2. The reason for this reduction could be the excessive time of arc application [48-51], which leads to the evaporation of Al and Si, resulting in less molten Al and eutectic fluid being formed, and less Ti_3SiC_2 being synthesized as heat and mass transfer decrease.

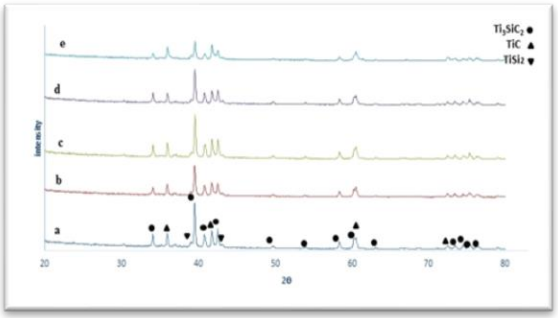

Fig. 10. XRD pattern of 3Ti:1.2SiC:0.8C:0.1Al mixture under arc melting at a) 1, b) 3, c) 5 d) 10 and e) 15s

The XRD pattern of the samples containing 3Ti:1.2SiC:0.8C:0.3Al under arc melting at 1, 3, 5, and 10s is shown in Fig. 11. As can be seen, in addition to Ti_3SiC_2, TiC, and $TiSi_2$ peaks, low-intensity Ti_5Si_3 peaks have been identified in all samples. Due to the increase of Al% in the initial mixture, the distance between Ti particles and carbon has increased. By setting arc for 1s (Fig. 11-a), Al melts and fills the gaps among the particles, improving heat and mass transfer for the reaction between Ti and carbon and the formation of TiC. However, because the arc application time is short, the obtained TiC particles do not have the opportunity to react with the eutectic fluid, so the peak intensity of TiC is much higher than the peak intensity of Ti_3SiC_2. Fig. 11-b shows that the peak intensity of TiC has decreased sharply compared to Fig. 11-a, but the peak intensity of Ti_3SiC_2 has had a relative increase. In Fig. 11-c the peak intensity of Ti_3SiC_2 has increased compared to Fig. 11-b, which can be due to the greater reaction of TiC and Ti_5Si_3 particles with eutectic liquid. In this Fig. the $TiSi_2$ peak disappears and it seems that there is no additional Si to react with Ti. As shown in Fig. 11-d, the main peak of Ti_3SiC_2 decreased, the main peak of TiC increased and the peak of Ti_5Si_3 also had a relative increase. With increasing the arc melting time, Si and Al evaporate [52-55]. Due to the high percentage of Al in the initial mixture, there are fewer particles to react with when Al evaporates; Thus, less Ti_3SiC_2 is obtained. Due to the layered structure of the Ti_3SiC_2 (TiC blocks separated by Si), the lack of Si has led to its decomposition. In addition, at high temperatures, with carbon penetration, Ti_3SiC_2 silicium plates are substituted with carbon plates and TiC is formed. Accordingly, the TiC peak has increased. According to the two-phase Ti and Si diagram, it can be predicted that the relative increase of the Ti5Si3 peak in Fig. 11-d is because of silicon deficiency in some parts of the sample.

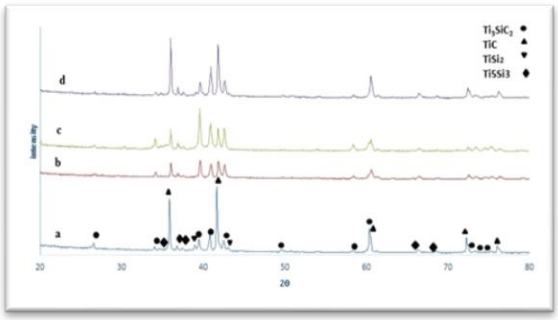

Fig. 11. XRD pattern of 3Ti:1.2SiC:0.8C:0.3Al mixture under arc melting at a) 1, b) 3, c) 5 and d) 10s

Table 3 shows the weight percentage of the Ti_3SiC_2 and TiC phases of the samples. As can be seen, the maximum purity of Ti_3SiC_2 for samples without Al is 60.33 wt%. In samples containing 0.1 Al, with increasing arc time up to 5 s, the weight percentage of Ti_3SiC_2 was relatively high and almost unchanged, and at longer arc times, its value decreased. In samples containing 0.3Al, the purity of Ti_3SiC_2 increases up to 80.5 wt% with increasing arc time up to 5 s, and the purity of Ti_3SiC_2 decreases with a further increase of arc time. As the arc time increases to 5s due to the

application of additional energy, the more eutectic liquid phase is produced, and as a result the reaction between TiC and the eutectic liquid phase increases, and finally more Ti_3SiC_2 is synthesized.

Table 3. Quantitative analysis of samples

Sample No.	Tic (wt.%)	Ti_3SiC_2 (wt.%)
1	47.5	52.5
2	43	57
3	41.8	58.20
4	39.67	60.33
5	18.56	81.44
6	17.7	82.3
7	16.4	83.6
8	20.6	79.4
9	27.67	72.33
10	72.2	27.8
11	30.7	69.3
12	19.5	80.5
13	65.6	34.4

3.3. Morphology of synthesized Ti3SiC2

Fig. 12 shows the FE-SEM images for the sample in Example 1. Fig. 12(a) shows particles of different sizes on a layered structure with approximately equal distances between layers. Due to the coaxial growth of the layered structure, the eutectic liquid phase and molten Al particles may have provided a suitable foundation for the germination and growth of Ti_3SiC_2 grains [56]. Figures 12(b) and 12(c) show the magnifications of sections 1 and 2 specified in Fig. 12(a), respectively, which depict the layered structure more clearly.

Fig. 13 and Table 4 show the EDS analysis of points A, D, B and C identified in Figures 12(b) and 12(c). In Fig. 13(a) which is related to point A, the carbon element peak is not seen in the images due to its proximity to zero. But in Table 4 of the analysis, its weight percentage has been mentioned. According to the EDS analysis images at point A and the presence of Al and Si with Ti,the formed phase is a solid solution of $Ti_3Si_{1-x}Al_xC_2$ [22, 23]. According to Fig. 13(b) and Table 4 related to point D, the particle specified in the figure can be considered as a combination of TiC, $TiSi_2$, and $TiAl_3$. Excess Al can react with Ti to form $TiAl_3$. However, this compound is not detected in XRD patterns due to the overlap of the $TiAl_3$ peak with other phases [22, 23]. Fig. 13(c) and the numbers in Table 4 for point B show that the particle specified in Figure can be considered as a combination of TiC, $TiSi_2$, and $TiAl_3$. Regarding point C, according to Fig. 13(d) and Table 4 and also according to the layered structure of point C, the formed phase can be considered as a solid solution of $Ti_3Si_{1-x}Al_xC_2$.

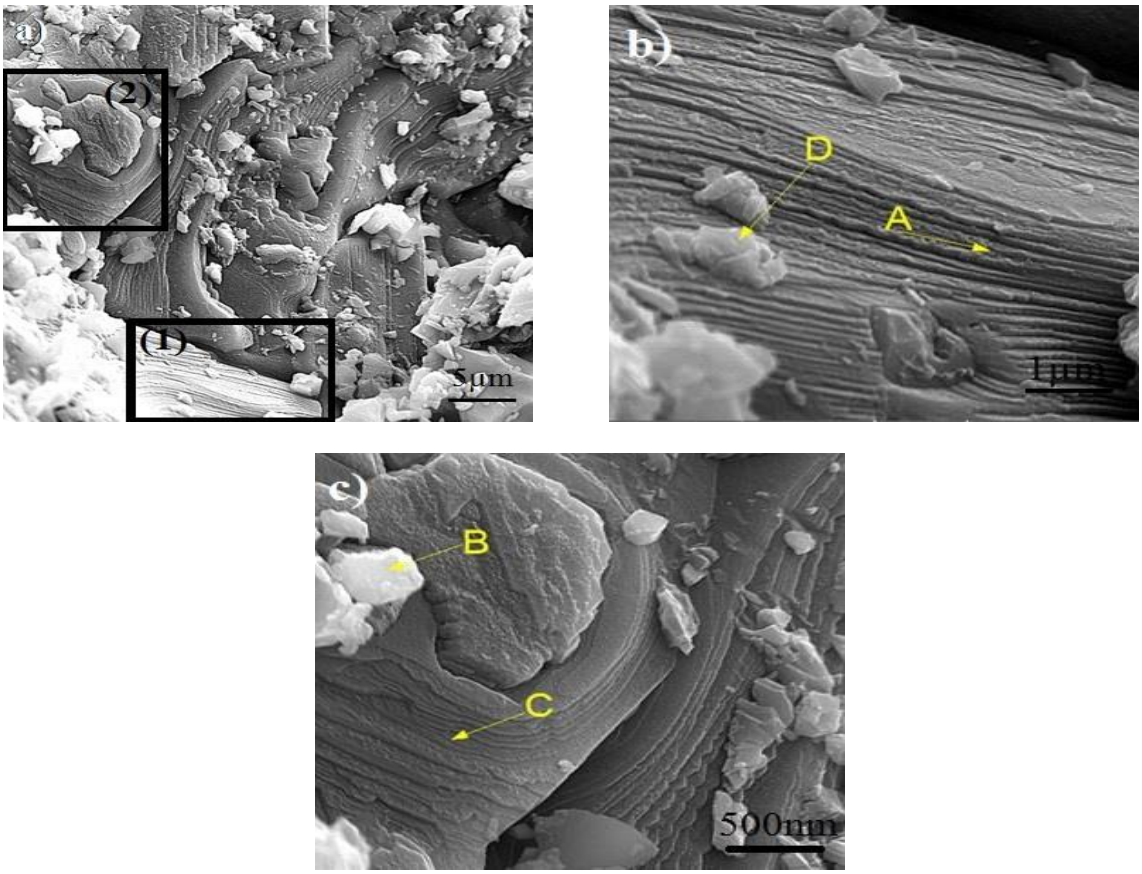

Fig. 12. (a) SEM images for a synthesized powder with a molar ratio of 3Ti:1.2SiC:0.8C:0.1Al and an arc melting time of 5s; (b) magnification of area (1) from Fig. 12(a); (c) magnification of area (2) from Fig. 12(a)

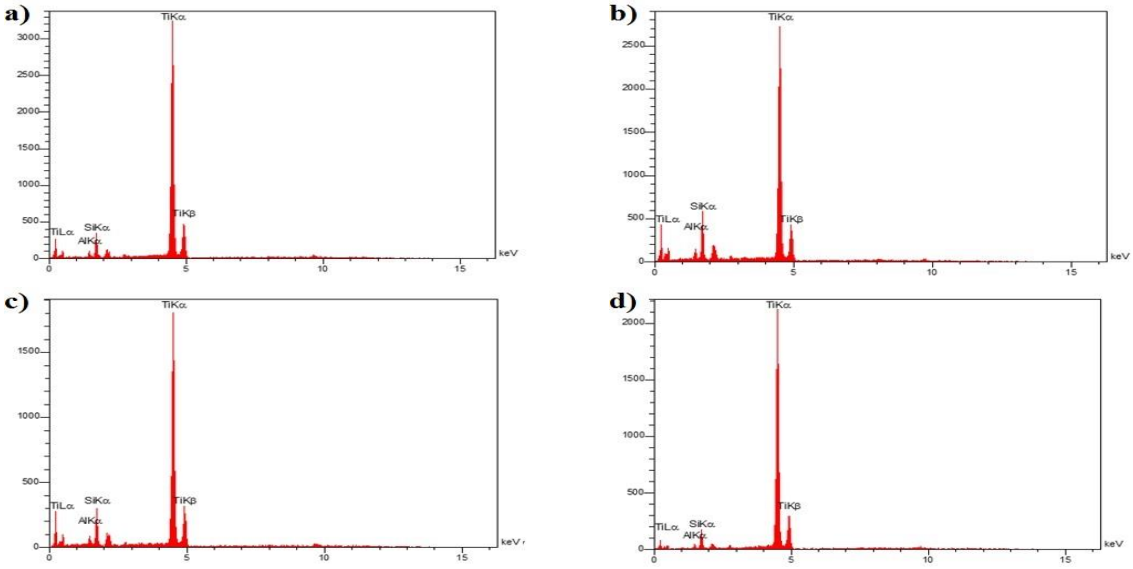

Fig. 13. EDS analysis images of the points specified in Figures 12(b) and 12(c) point; (a) A, (b) D, (c) B, and (d) C

Table 4. Quantitative analysis of points A, D, B, and C specified in Figures 12(b) and 12(c)

Material \ Point	Al	C	Si	Ti
A	0.47	10.42	2.02	75.59
D	0.8	15.86	2.87	65.43
B	0.75	14.91	3.63	64.37
C	0.44	4.48	1.82	84.66

Fig. 14. The SEM image shows Fig. 12(a). Given the uniform contrast of the layered regions and the results of the XRD patterns and EDS analysis images, these areas are considered to be a solid solution of $Ti_3Si_{1-x}Al_xC_2$.

Fig. 14. SEM image of a synthesized powder with a molar ratio of 3Ti:1.2SiC:0.8C: 0.1Al and an arc time of 5s.

Fig. 15 shows the SEM images of the synthesized sample containing 3Ti:1.2SiC: 0.8C: 0.3Al and an arc time of 5s. According to Fig. 18-a the layered structure is observed; but most particles are Nub-like. Also, according to the results of XRD patterns, it can be estimated that this layered structure is related to the Ti_3SiC_2 phase. Comparing Figures 12(a) and 15, it can be seen that with increasing Al, the shape of most particles changes from layered to fragmented and massive.

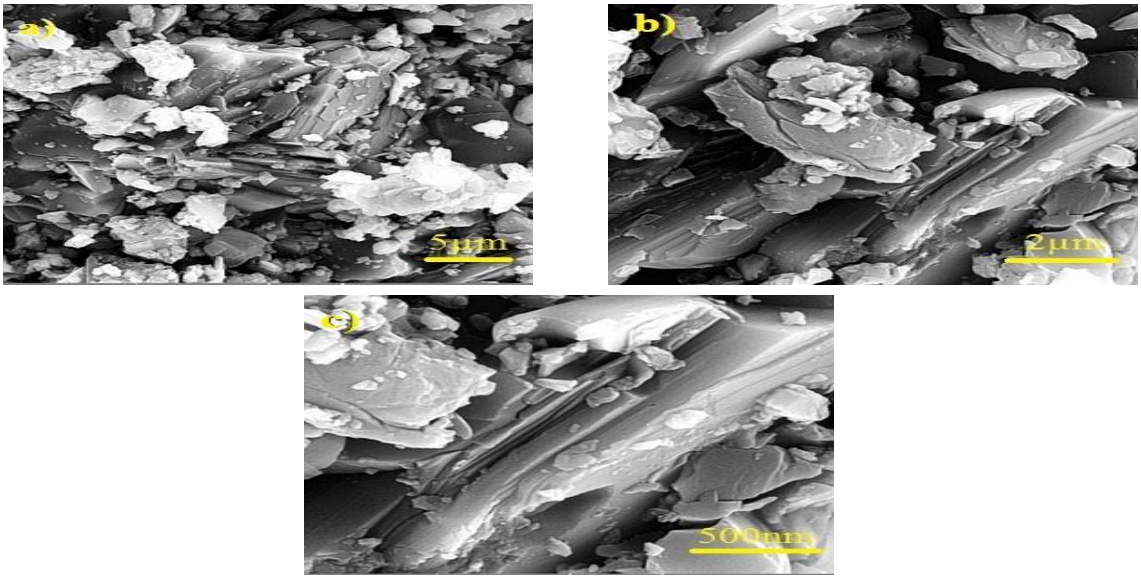

Fig. 15. SEM images for synthesized powder with 3Ti:1.2SiC:0.8C:0.3Al molar ratio and 5s arc time at magnifications (a) 5μm, (b) 2μm, (c) 500nm

4. Conclusion

In this study, the optimal values of arc melting duration parameters and mixing ratio of Ti/SiC/Al/graphite raw materials in Ti_3SiC_2 powder synthesis have been investigated. Hence, the following results were obtained:

- The optimal time for the synthesis of Ti_3SiC_2 by arc melting method is for the mixture of primary powders containing Al at 5s, and at a longer time, the amount of Ti_3SiC_2 is reduced. Its purity in samples of 3Ti:1.2SiC:0.8C:0.1Al and 3Ti:1.2SiC:0.8C:0.3Al is equal to 83.6wt% and 80.5 wt%, respectively.
- Adding Al to the initial powder mixture can increase the percentage of Ti_3SiC_2 phase to more than 23 wt.% in the final product.
- In the initial powder mixture with a molar ratio of 3Ti:1.2SiC:0.8C, the purity of the synthesized Ti_3SiC_2 increases with increasing arc melting time. The highest percentage of synthesized Ti_3SiC_2 was 60.33 wt%, which is related to the 10s arc melting time.

Conflicts of Interest

The authors declare that there is no conflict of interest regarding the publication of this paper.

References

[1] Foratirad, H., Baharvandi, H. and Maraghe, M.G., 2017. Effect of excess silicon content on the formation of nano-layered Ti3SiC2 ceramic via infiltration of TiC preforms. *Journal of the European ceramic society*, *37*(2), pp.451-457.

[2] Atazadeh, N., Heydari, M.S., Baharvandi, H.R. and Ehsani, N., 2016. Reviewing the effects of different additives on the synthesis of the Ti3SiC2 MAX phase by mechanical alloying technique. *International Journal of Refractory Metals and Hard Materials*, *61*, pp.67-78.

[3] Pourebrahim, A., Baharvandi, H., Foratirad, H. and Ehsani, N., 2018. Effect of aluminum addition on the densification behavior and mechanical properties of synthesized high-purity nano-laminated Ti3SiC2 through spark plasma sintering. *Journal of Alloys and Compounds*, *730*, pp.408-416.

[4] Pourebrahim, A., Baharvandi, H., Foratirad, H. and Ehsani, N., 2019. Low temperature synthesis of high-purity Ti3SiC2 via additional Si through spark plasma sintering. *Journal of Alloys and Compounds*, *789*, pp.313-322.

[5] Yaghobizadeh, O., Sedghi, A. and Baharvandi, H.R., 2019. Effect of Ti3SiC2 on the ablation behavior and mechanism of Cf-C-SiC-Ti3SiC2 composites under oxyacetylene torch at 3000° C. *Ceramics International*, *45*(1), pp.777-785.

[6] Dash, A., Vaßen, R., Guillon, O. and Gonzalez-Julian, J., 2019. Molten salt shielded synthesis of oxidation prone materials in air. *Nature materials*, *18*(5), pp.465-470.

[7] Barsoum, M.W. and Radovic, M., 2011. Elastic and mechanical properties of the MAX phases. *Annual review of materials research*, *41*, pp.195-227.

[8] Sokol, M., Natu, V., Kota, S. and Barsoum, M.W., 2019. On the chemical diversity of the MAX phases. Trends in Chemistry, 1(2), pp.210-223.

[9] Clark, D.W., Zinkle, S.J., Patel, M.K. and Parish, C.M., 2016. High temperature ion irradiation effects in MAX phase ceramics. Acta Materialia, 105, pp.130-146.

[10] Eklund, P., Beckers, M., Jansson, U., Högberg, H. and Hultman, L., 2010. The Mn+ 1AXn phases: Materials science and thin-film processing. *Thin Solid Films*, *518*(8), pp.1851-1878.

[11] Shih, C., Meisner, R., Porter, W., Katoh, Y. and Zinkle, S.J., 2013. Physical and thermal mechanical characterization of nonirradiated MAX phase materials (Ti-Si-C and Ti-Al-C systems). *Fusion Reactor Materials Program*, 55, pp.78-93.

[12] Barsoum, M.W., El-Raghy, T., Rawn, C.J., Porter, W.D., Wang, H., Payzant, E.A. and Hubbard, C.R., 1999. Thermal properties of Ti3SiC2. *Journal of Physics and Chemistry of Solids*, 60(4), pp.429-439.

[13] Liang, B.Y., Jin, S.Z. and Wang, M.Z., 2008. Low-temperature fabrication of high purity Ti3SiC2. *Journal of Alloys and Compounds*, *460*(1-2), pp.440-443.

[14] Ghosh, N.C. and Harimkar, S.P., 2013. Phase analysis and wear behavior of in-situ spark plasma sintered Ti3SiC2. *Ceramics International*, *39*(6), pp.6777-6786.

[15] Zhang, H., Wang, J., Wang, J., Zhou, Y., Peng, S. and Long, X., 2013. Role of nanolaminated crystal structure on the radiation damage tolerance of Ti3SiC2: theoretical investigation of native point defects. *Journal of Nanomaterials*, *2013*.

[16] Abderrazak, H., Turki, F., Schoenstein, F., Abdellaoui, M. and Jouini, N., 2013. Influence of mechanical alloying on Ti3SiC2 formation via spark plasma sintering technique from Ti/SiC/C powders. *Ceramics International*, *39*(5), pp.5365-5372.

[17] Abderrazak, H., Turki, F., Schoenstein, F., Abdellaoui, M. and Jouini, N., 2012. Effect of the mechanical alloying on the Ti3SiC2 formation by spark plasma sintering from Ti/Si/C powders. *International Journal of Refractory Metals and Hard Materials*, *35*, pp.163-169.

[18] Zou, Y., Sun, Z., Tada, S. and Hashimoto, H., 2008. Effect of liquid reaction on the synthesis of Ti3SiC2 powder. *Ceramics international*, *34*(1), pp.119-123.

[19] Peng, M., Shi, X., Zhu, Z., Wang, M. and Zhang, Q., 2012. Facile synthesis of Ti3SiC2 powder by high energy ball-milling and vacuum pressureless heat-treating process from Ti–TiC–SiC–Al powder mixtures. *Ceramics International*, *38*(3), pp.2027-2033.

[20] Meng, F., Chaffron, L. and Zhou, Y., 2009. Synthesis of Ti3SiC2 by high energy ball milling and reactive sintering from Ti, Si, and C elements. *Journal of Nuclear Materials*, *386*, pp.647-649.

[21] Hashimoto, H., Sun, Z.M. and Tada, S., 2007. Morphological evolution during reaction sintering of Ti, SiC and C powder blend. *Journal of alloys and compounds*, *441*(1-2), pp.174-180.

[22] Yongming, L., Zhimin, Z., Caihong, X. and Xuening, M., 2008. Polycarbosilane derived Ti3SiC2. *Materials Letters*, *62*(20), pp.3570-3572.

[23] Yang, J., Zhang, X., Wang, Z., He, P., Gao, L. and Dong, S., 2012. Fabrication of Ti3SiC2 powders using TiH2 as the source of Ti. *Ceramics International*, *38*(4), pp.3509-3512.

[24] Yeh, C.L. and Shen, Y.G., 2008. Effects of TiC addition on formation of Ti3SiC2 by self-propagating high-temperature synthesis. *Journal of Alloys and Compounds*, *458*(1-2), pp.286-291.

[25] El Saeed, M.A., Deorsola, F.A. and Rashad, R.M., 2012. Optimization of the Ti3SiC2 MAX phase synthesis. *International Journal of Refractory Metals and Hard Materials*, *35*, pp.127-131.

[26] Shan, D., Yan, G., Zhou, L., Li, C., Li, J., Liu, G. and Feng, J., 2011. Synthesis of Ti3SiC2 bulks by infiltration method. *Journal of alloys and compounds*, *509*(8), pp.3602-3605.

[27] Hwang, S.S., Han, J., Lee, D. and Park, S.W., 2011. Synthesis of Ti3SiC2 by infiltration of molten Si. *Journal of alloys and compounds*, *509*(35), pp. L336-L339.

[28] Sun, Z., Yang, S. and Hashimoto, H., 2007. Effect of Al on the synthesis of Ti3SiC2 by reactively sintering Ti–SiC–C powder mixtures. *Journal of alloys and compounds*, *439*(1-2), pp.321-325.

[29] Zou, Y., Sun, Z., Hashimoto, H. and Cheng, L., 2010. Reaction mechanism in Ti–SiC–C powder mixture during pulse discharge sintering. *Ceramics International*, *36*(3), pp.1027-1031.

[30] Gubarevich, A.V., Tamura, R., Maletaskić, J., Yoshida, K. and Yano, T., 2019. Effect of aluminium addition on yield and microstructure of Ti3SiC2 prepared by combustion synthesis method. *Materials Today: Proceedings*, *16*, pp.102-108.

[31] Yongming, L., Wei, P., Shuqin, L., Jian, C., Ruigang, W. and Jianqiang, L., 2002. Synthesis of high-purity Ti3SiC2 polycrystals by hot-pressing of the elemental powders. *Materials Letters*, *52*(4-5), pp.245-247.

[32] Antti, M.L., Kero, I., Cheng, Y.B. and Tegman, R., 2012. Phase reactions in a hot-pressed TiC/Si powder mixture. *Ceramics International*, *38*(3), pp.1999-2003.

[33] Wu, Q., Li, C. and Tang, H., 2010. Surface characterization and growth mechanism of laminated Ti3SiC2 crystals fabricated by hot isostatic pressing. *Applied surface science*, *256*(23), pp.6986-6990.

[34] Pickering, E., Lackey, W.J. and Crain, S., 2000. CVD of Ti3SiC2. *Chemical Vapor Deposition*, *6*(6), pp.289-295.

[35] Sun, Z., Hashimoto, H., Tian, W. and Zou, Y., 2010. Synthesis of the MAX phases by pulse discharge sintering. *International Journal of Applied Ceramic Technology*, *7*(6), pp.704-718.

[36] Yang, S., Sun, Z., Yang, Q. and Hashimoto, H., 2007. Effect of Al addition on the synthesis of Ti3SiC2 bulk material by pulse discharge sintering process. *Journal of the European Ceramic Society*, *27*(16), pp.4807-4812.

[37] Li, Z., Wei, X., Luo, F., Zhou, W. and Hao, Y., 2014. Microwave dielectric properties of Ti3SiC2 powders synthesized by solid state reaction. *Ceramics International*, *40*(1), pp.2545-2549.

[38] Hosseinizadeh, S.A., Pourebrahim, A., Baharvandi, H. and Ehsani, N., 2020. Synthesis of nano-layered Ti3SiC2 MAX phase through reactive melt infiltration (RMI): Metallurgical and thermodynamical parameters. *Ceramics International*, *46*(14), pp.22208-22220.

[39] Klemm, H., Tanihata, K. and Miyamoto, Y., 1992. Gas Pressure Combustion Sintering of Materials in the Ti-Si-C-System. In *Hot Isostatic Pressing—Theory and Applications* (pp. 451-456). Springer, Dordrecht.

[40] Zhang, Y., Zhou, Y.C. and Li, Y.Y., 2003. Solid–liquid synthesis of Ti3SiC2 particulate by

fluctuation procedure. *Scripta materialia*, *49*(3), pp.249-253.

[41] Abu, M.J., Mohamed, J.J. and Ahmad, Z.A., 2012. Effect of excess silicon on the formation of Ti3SiC2 using free Ti/Si/C powders synthesized via arc melting. *International Scholarly Research Notices*, *2012*.

[42] Sun, Z.M., 2011. Progress in research and development on MAX phases: a family of layered ternary compounds. *International Materials Reviews*, *56*(3), pp.143-166.

[43] Barsoum, M.W., El-Raghy, T. and Ali, M., 2000. Processing and characterization of Ti2AlC, Ti2AlN, and Ti2AlC0. 5N0. 5. *Metallurgical and Materials Transactions A*, *31*(7), pp.1857-1865.

[44] Sun, Z., Zou, Y., Tada, S. and Hashimoto, H., 2006. Effect of Al addition on pressureless reactive sintering of Ti3SiC2. *Scripta materialia*, *55*(11), pp.1011-1014.

[45] Sun, Z., Yang, S. and Hashimoto, H., 2004. Ti3SiC2 powder synthesis. *Ceramics International*, *30*(7), pp.1873-1877.

[46] Istomin, P., Istomina, E., Nadutkin, A., Grass, V., Leonov, A., Kaplan, M. and Presniakov, M., 2017. Fabrication of Ti3SiC2 and Ti4SiC3 MAX phase ceramics through reduction of TiO2 with SiC. *Ceramics International*, *43*(18), pp.16128-16135.

[47] Salmany Kozekanan, B., Moradkhani, A., Baharvandi, H. and Ehsani, N., 2021. Mechanical properties of SiC-C-B4C composites with different carbon additives produced by pressureless sintering. *International Journal of Applied Ceramic Technology*, *18*(3), pp.957-971.

[48] FarahBakhsh, I., Antiochia, R. and Jang, H.W., 2021. Pressureless sinterability study of ZrB2–SiC composites containing hexagonal BN and phenolic resin additives. *Synthesis and Sintering*, *1*(2), pp.99-104.

[49] Nayebi, B., Asl, M.S., Akhlaghi, M., Ahmadi, Z., Tayebifard, S.A., Salahi, E., Shokouhimehr, M. and Mohammadi, M., 2021. Spark plasma sintering of TiB2-based ceramics with Ti3AlC2. *Ceramics International*, *47*(9), pp.11929-11934.

[50] Amiri, S.H., Kakroudi, M.G., Vafa, N.P. and Asl, M.S., 2022. Synthesis and Sintering of Ti3SiC2–SiC Composites through Reactive Hot-Pressing of TiC and Si Precursors. *Silicon*, *14*(8), pp.4227-4235.

[51] Asl, M.S., Nayebi, B., Akhlaghi, M., Ahmadi, Z., Tayebifard, S.A., Salahi, E., Shokouhimehr, M. and Mohammadi, M., 2021. A novel ZrB2-based composite manufactured with Ti3AlC2 additive. *Ceramics International*, *47*(1), pp.817-827.

[52] Mansoor, M., Mansoor, M., Mansoor, M., Er, Z. and Şahin, F.Ç., 2021. Ab-initio study of paramagnetic defects in Mn and Cr doped transparent polycrystalline Al2O3 ceramics. *Synthesis and Sintering*, *1*(3), pp.135-142.

[53] Amiri, S.H., Kakroudi, M.G., Rabizadeh, T. and Asl, M.S., 2020. Characterization of hot-pressed Ti3SiC2–SiC composites. *International Journal of Refractory Metals and Hard Materials*, *90*, p.105232.

[54] Akhlaghi, M., Tayebifard, S.A., Salahi, E., Asl, M.S. and Schmidt, G., 2018. Self-propagating high-temperature synthesis of Ti3AlC2 MAX phase from mechanically-activated Ti/Al/graphite powder mixture. *Ceramics International*, *44*(8), pp.9671-9678.

[55] Salari, M.A., Muğlu, G.M., Rezaei, M., Kumar, M.S., Pulikkalparambil, H. and Siengchin, S., 2021. In-situ synthesis of TiN and TiB2 compounds during reactive spark plasma sintering of BN–Ti composites. *Synthesis and Sintering*, *1*(1), pp.48-53.

[56] Akhlaghi, M., Tayebifard, S.A., Salahi, E. and Asl, M.S., 2018. Spark plasma sintering of TiAl–Ti3AlC2 composite. *Ceramics International*, *44*(17), pp.21759-21764.